

Article

New Dinosaur Ichnological, Sedimentological, and Geochemical Data from a Cretaceous High-Latitude Terrestrial Greenhouse Ecosystem, Nanushuk Formation, North Slope, Alaska

Anthony R. Fiorillo ^{1,*}, Paul J. McCarthy ², Grant Shimer ³, Marina B. Suarez ⁴, Ryuji Takasaki ⁵, Tsogtbaatar Chinzorig ⁶, Yoshitsugu Kobayashi ⁷, Paul O'Sullivan ⁸ and Eric Orphys ²

¹ New Mexico Museum of Natural History & Science, Albuquerque, NM 87104, USA

² Department of Geosciences, Geophysical Institute, University of Alaska Fairbanks, Fairbanks, AK 99775-5780, USA; pjmccarthy@alaska.edu (P.J.M.); ejorphys@alaska.edu (E.O.)

³ Department of Geosciences, Southern Utah University, Cedar City, UT 84720, USA; grantshimer@suu.edu

⁴ Department of Geology, University of Kansas, Lawrence, KS 66045, USA; mbsuarez@ku.edu

⁵ Department of Ecology and Evolutionary Biology, University of Toronto, Toronto, ON M5S 1A1, Canada

⁶ North Carolina Museum of Natural Sciences, Raleigh, NC 27601, USA; ctsoqtb@ncsu.edu

⁷ Hokkaido University Museum, Hokkaido University, Sapporo 060-0810, Japan

⁸ GeoSep Services, Moscow, ID 83843, USA

* Correspondence: anthony.fiorillo@dca.nm.gov

Abstract: The Nanushuk Formation (Albian–Cenomanian) crops out over much of the central and western North Slope of Alaska, varying from ≈ 1500 to ≈ 250 m thick from west to northeast. The Nanushuk Formation records an inter-tonguing succession of marine and nonmarine conglomerate, sandstone, mudstone, and coal. These rock units comprise the Kukpowruk and Corwin formations of the former Nanushuk Group, respectively. Work presented here is centered in the foothills of the DeLong Mountains along the Kukpowruk River, from an area west of Igloo Mountain in the Coke Basin to the Barabara Syncline, approximately 80 km to the north. A radiometric date recovered from a tuff in our study area suggests a Cenomanian age for at least some of these rocks. Outcrops along the Kukpowruk River contain a well-preserved fossil flora previously recovered from marine, marginal marine, and terrestrial sediments. Our own work focuses on detailed measured sections of terrestrial rocks, interpretation of sedimentary facies and facies associations, and documentation of fossil vertebrates. Eight facies associations are identified in the study area that together are interpreted to represent meandering fluvial and upper delta plain environments. Plant fossils are common and include standing tree trunks up to 58 cm in diameter at some locations. Approximately 75 newly discovered tracksites, and a heretofore unknown, rich fossil vertebrate ichnofauna, are present. The ichnofaunal assemblage includes evidence of small and large theropod dinosaurs (including birds) and bipedal and quadrupedal ornithischian dinosaurs. Approximately 15% of the dinosaur ichnofauna record is represented by fossil bird tracks. Wood fragments from the Nanushuk Formation were analyzed for their carbon isotopic composition to relate $\delta^{13}\text{C}$ to mean annual precipitation. Samples averaged -26.4% VPDB, suggesting an average MAP of 1412 mm/year. This record of increased precipitation in the Nanushuk Fm. during the mid-Cretaceous provides new data that supports global precipitation patterns associated with the Cretaceous Thermal Maximum. This work provides an important framework for much-needed further paleoecological and paleoclimatic analyses into greenhouse conditions in the terrestrial Cretaceous Arctic during this important window in time.

Keywords: dinosaurs; footprints; paleosols; paleoecology; paleoenvironments



Citation: Fiorillo, A.R.; McCarthy, P.J.; Shimer, G.; Suarez, M.B.; Takasaki, R.; Chinzorig, T.; Kobayashi, Y.; O'Sullivan, P.; Orphys, E. New Dinosaur Ichnological, Sedimentological, and Geochemical Data from a Cretaceous High-Latitude Terrestrial Greenhouse Ecosystem, Nanushuk Formation, North Slope, Alaska. *Geosciences* **2024**, *14*, 36. <https://doi.org/10.3390/geosciences14020036>

Academic Editor: Jesus Martinez-Frias

Received: 13 December 2023

Revised: 23 January 2024

Accepted: 26 January 2024

Published: 30 January 2024



Copyright: © 2024 by the authors. Licensee MDPI, Basel, Switzerland. This article is an open access article distributed under the terms and conditions of the Creative Commons Attribution (CC BY) license (<https://creativecommons.org/licenses/by/4.0/>).

1. Introduction

It is a truism that the pace of human-caused changes to global climate is increasingly overwhelming ecosystems that have, in general, been relatively stable over several thou-

sands of years. As the world's human population continues to explode in size at the same time as rapid climate change, it is forcing a reshaping of conservation paradigms that now include looking to the past for guidance on crucial aspects of ecosystems and their health [1]. The prevailing conservation paradigm has been to hold ecosystems to a now appreciated unrealistic idealized model of stasis. But now it is becoming clear that new approaches using historical as well as novel landscapes provide insights into key issues such as drivers of biodiversity, fundamental processes within ecosystems, and the interplay between biota and climate [2–4]. Sedimentary rocks from the Late Cretaceous Arctic and sub-Arctic present an opportunity to assess ecosystems that existed during an extreme planetary greenhouse condition.

The mid to Late Cretaceous of Alaska represents one of these time periods with terrestrial Cretaceous deposits ranging from the Albian to the Maastrichtian. While much work has been advanced for the Late Cretaceous Polar Arctic (Prince Creek Formation), detailed reconstruction of the mid-Cretaceous Nanushuk Formation still requires a comprehensive and quantitative approach. The Albian–Cenomanian of Alaska was arguably warmer than the Late Cretaceous Polar Arctic [5,6]. More broadly, the mid-Cretaceous was also a period of global environmental and evolutionary change that included rising sea levels, diversification of flowering plants, and vertebrate faunal diversification and turnover [7–10].

The Albian–Cenomanian time was the earliest episode of faunal exchange between Beringia and Asia, e.g., [11]. This route between the North American and Asian continents has repeatedly been key to the dispersal of organisms starting during the time represented by the Nanushuk Formation up to the more recent Pleistocene faunal exchanges. While the Nanushuk Formation is prominent across all of northern Alaska, this study focuses on exposures of the unit along the Kukpowruk River in far northwestern Alaska (Figure 1). Here, we build on the detailed earlier paleobotanical survey work by Spicer and Herman [12] and provide new sedimentological, paleontological, and paleoclimatological data for this region. While their seminal work [12] provided needed insights into floral communities ranging from marsh/heath communities to forested river margin communities found along the Kukpowruk River, their study did not provide information on fossil vertebrates and paleoclimate, with only limited sedimentological detail. As such, this study takes the first major steps to improve our understanding of this critical window in deep time.

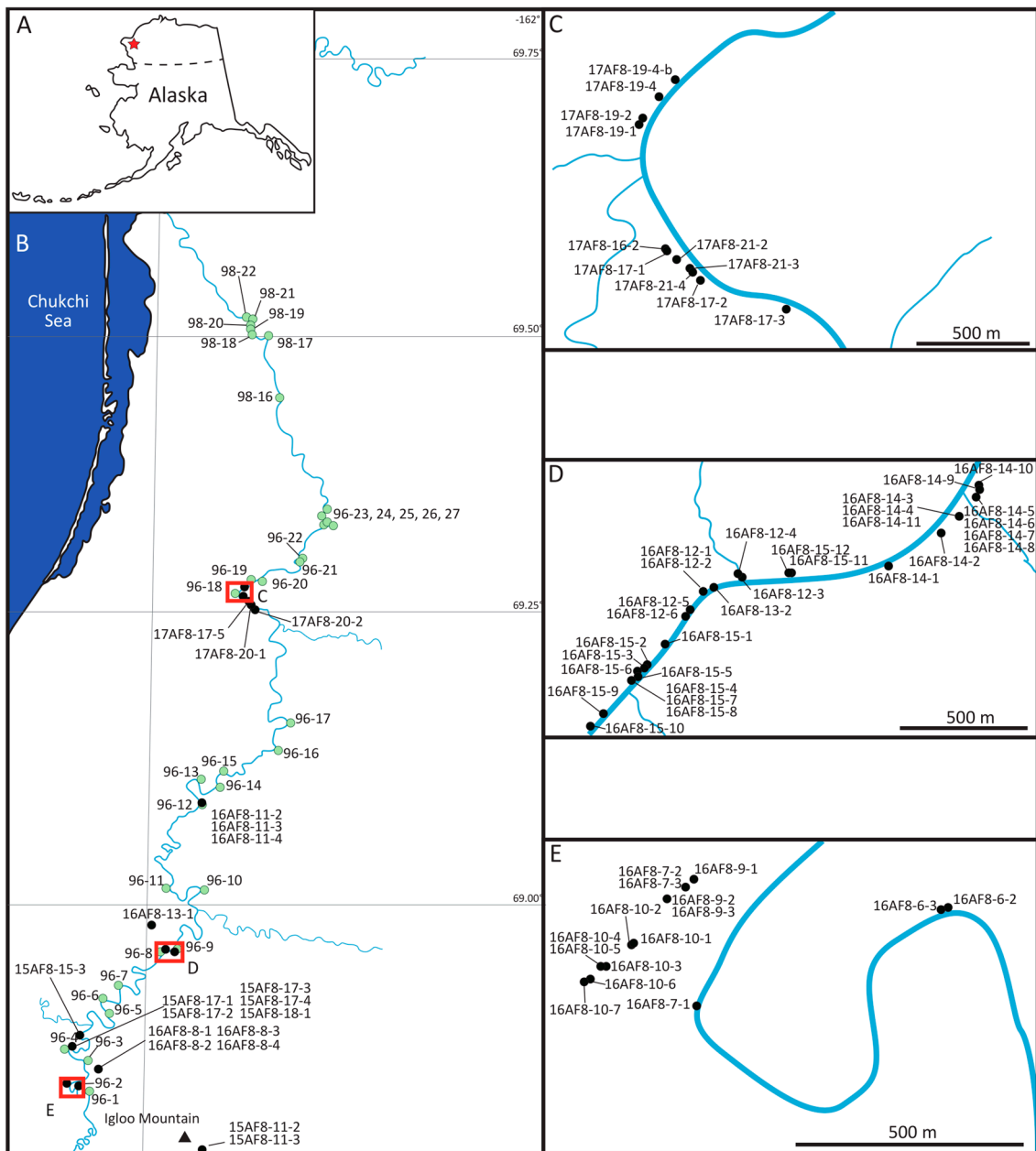


Figure 1. (A) Map of Alaska with a star showing location of study area. (B) Map of Kukpowruk River showing locations of fossil vertebrate tracksites (designated by combination of numbers and letters) in this study, and fossil plant sites (designated by only numbers) from study by Spicer and Herman [12]. (C–E) More detailed maps of areas of high concentration of fossil footprint sites.

2. Geologic Framework

The Nanushuk Fm. and coeval upper Torok Fm. fill the western part of a large, east–west trending, peripheral foreland basin across the west-central North Slope of Alaska. The basin is bounded to the south by the Brooks Range fold and thrust belt [13]. The fold and thrust belt comprises a succession of sedimentary rocks thrust northward that are partly contemporaneous with rifting on the northern flank [13,14]. The Colville foreland basin formed due to the load imposed by thrust faulted allochthons within the growing Cretaceous Brooks Range, followed by sediment deposition eroded from them. Orogen-wide uplift and erosion between 135–95 Ma resulted in the deposition of clastic sediments to the north and northeast, including early Albian to Cenomanian fluvial–deltaic strata of the Nanushuk Fm. [15,16].

The Nanushuk Fm. and upper Torok Fm. are present in the northern foothills belt and in the subsurface of the North Slope coastal plain (Figure 2). The Nanushuk Fm. is a succession of inter-tonguing marine and nonmarine rocks interpreted as marine shelf, delta plain, strandplain, fluvial, and alluvial overbank deposits [14–23]. Mull et al. [24] revised the stratigraphy of the Albian–Cenomanian Nanushuk Group, which included the marine Tuktu, Grandstand, and Ninuluk formations, the predominantly nonmarine Chandler and Corwin formations, and the marine–nonmarine Kukpowruk Formation. Mull et al. [24] downgraded the Nanushuk Group to formation status, incorporating all six formations of the former Nanushuk Group. Thickness estimates for the Nanushuk Fm. range from 2750 m along the Chukchi Sea coast in the west [21] to a zero edge \approx 75 km east of Umiat, and in the vicinity of the modern Colville delta. The Nanushuk Fm. crops out in the northern Brooks Range foothills belt and coastal plain, comprising a lower dominantly marine unit of inter-tonguing shallow-marine shale, siltstone, and sandstone (Tuktu and Grandstand formations of former usage), that grades to the north to east-northeast into outer-shelf, slope, basinal shale, and minor sandstone of the upper Torok Fm. [15,16]. This grades up-section into primarily nonmarine mudstone, coal, sandstone, and conglomerate (Chandler Formation of former usage). These nonmarine rocks intertongue with rocks representing coastal facies within the Nanushuk Fm. [15,16]. Overall, the Nanushuk Fm. comprises a thick regressive package, interrupted many times by marine flooding that resulted from delta lobe shifting and abandonment.

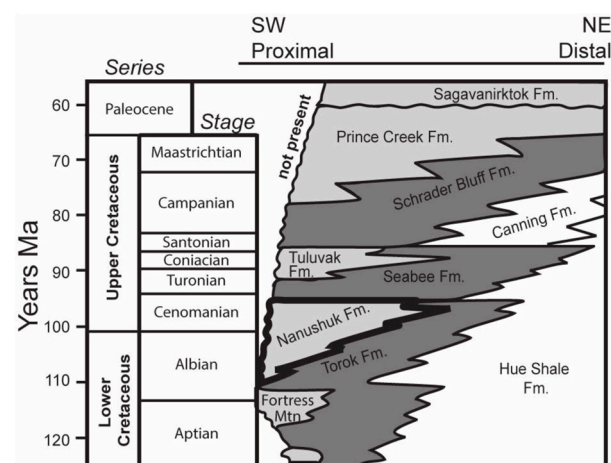


Figure 2. Stratigraphic nomenclature for Cretaceous and Paleocene rock units of the North Slope of Alaska.

Throughout the western North Slope of Alaska, an angular unconformity bounds the Nanushuk Fm., separating nonmarine Cretaceous rocks from overlying Pleistocene sediments. In the central North Slope and the subsurface of the eastern National Petroleum Reserve-Alaska (NPR), Cenomanian intertonguing fluvial sandstone, paludal mudstone and coal, and shallow-marine sandstone and silty shale overlies dominantly nonmarine Nanushuk rocks [15,25]. These 350 m thick intertonguing nonmarine and marine rocks were included in the Niakogon Tongue (Chandler Formation) and Ninuluk Formation of former usage, and now part of the Nanushuk Formation, and record a change from regression to regional transgression [25]. At outcrop and in the subsurface where the lower contact of the Nanushuk with the Seabee Fm. is present, the Seabee typically consists of a thin, basal transgressive lag of fine- to medium-grained sandstone a few cm to dm thick that grades into thin-bedded fine- to very fine-grained sandstone a few meters thick that is overlain by bentonite-rich mudstone. Alternatively, the basal lag may be abruptly overlain solely by bentonite-rich mudstone.

Alhbrandt et al. [21] recognized two major delta systems in the Nanushuk Fm.; the Corwin Delta, on the western side of the basin, and the Umiat Delta on the eastern side. Both

the Corwin and Umiat Deltas are not individual deltas, instead representing thick deltaic depocenters, or complexes, comprising the deposition of many individual delta lobes. Fisher et al. [18] suggested that the eastern delta was river dominated. Ahlbrandt et al. [21] and Huffman et al. [20] indicated that both delta complexes were river dominated, but they also suggested that the Umiat delta complex was affected by greater wave reworking. Recent work suggests that river- and wave-reworking of delta complexes varies temporally as well as spatially in the eastern Nanushuk Fm., with initial wave dominance followed by subsequent river influence in shallower, more wave-limited conditions created by earlier parasequence progradation and shelf construction [26].

Previous work indicates high mud and low sand contents in the Corwin delta complex [16,20,27], suggesting that the western delta complex was characterized by river-dominated delta lobes that prograded east-northeastward obliquely along the Colville basin axis [20,21,28]. In the Wainwright # 1 core to the northeast of our study area, LePain and Decker [28] documented lower and upper delta plain facies in the subsurface. Our outcrop facies analysis documents nonmarine sediments similar to their upper delta plain or alluvial plain facies. Biostratigraphic data indicates an early Albian to late Albian age for the Corwin Delta complex along the Chukchi Sea coast, which becomes younger in the east and north [19,21]. The Corwin delta complex dominated depositional patterns in the western two-thirds of the foreland basin [15] at a paleolatitude of $\approx 75^\circ$ N [29].

3. Radiometric Data from Study Area

LA-ICP-MS U-Pb zircon geochronology allows in situ grain spatial resolution [29] and high single grain resolution throughput (usually >100 grains per sample analysis), which is required for (a) dating complex zircons, (b) detrital studies, and (c) accurately dating bentonites with a potential detrital or xenolith component. Determining crystallization/eruption or maximum deposition age “calls” from LA-ICP-MS U-Pb zircon data are complicated by potential undetermined Pb loss for young zircons (<~400 Ma), matrix mismatch, and large N analysis resulting in apparently robust populations of younger grains that are just an artifact of instrumental statistical spread [30–32].

CA-ID-TIMS has higher accuracy and precision and can usually mitigate the effects of potential Pb loss [33], but this whole grain technique is time intensive, resulting in fewer grains analyzed per sample (usually ~3 to 7 grains) and no in situ grain spatial resolution. Hence, there is a tradeoff between LA-ICP-MS and CA-ID-TIMS U-Pb zircon dating applications. Many labs are now screening zircon grains via large N LA-ICP-MS U-Pb analysis and then performing CA-ID-TIMS U-Pb zircon analysis on select grains [34]. This dual-technique combination, though powerful, adds significant expense and time.

Furthermore, these dual-technique studies have demonstrated that selecting the LA-ICP-MS U-Pb zircon youngest statistical population (YSP), which is the weighted mean of the youngest statistical population (2 or more grains) that produces a mean square weighted deviation (MSWD) close to 1, approximates CA-ID-TIMS U-Pb zircon results from the same sample [35,36]. A variation of this approach is the youngest mode weighted mean (YMWM), which uses the LA-ICP-MS zircon dates that define the youngest age mode from a kernel density estimate peak that consists of at least three grains that overlap at 2 sigma uncertainty with an MSWD that approximates 1 [32,34]. We use a modified version of the YSP and YMWM age determinations by utilizing an iterative approach that captures the largest population of young grains that overlap at 2 sigma uncertainty with an MSWD that approximates 1. We call this approach the largest youngest statistical population (L-YSP) and favor it, because it allows the parsing of potential young tails that may have experienced Pb loss and older detrital and/or xenolith grains [37]. The results are often like those from Tuffzirc [38], which follows a similar approach, but uses a not-explained modified 2 sigma uncertainty overlap and can capture older grains that do not approximate depositional–eruption ages.

We applied a 10% uncertainty filter to remove less precise grains with possible isotopic/analytical concerns. We use the macro-spread sheet from Herriot et al. [36] to both

iteratively select grains and to calculate a weighted average age and systematic uncertainty. Based on the weighted average age of 34 out of 103 zircon grains dated, we determined an eruption age of 97.20 ± 0.53 with an MSWD of 0.98 for the bentonite sample 15-EQ-8-17-2 (Figure 3).

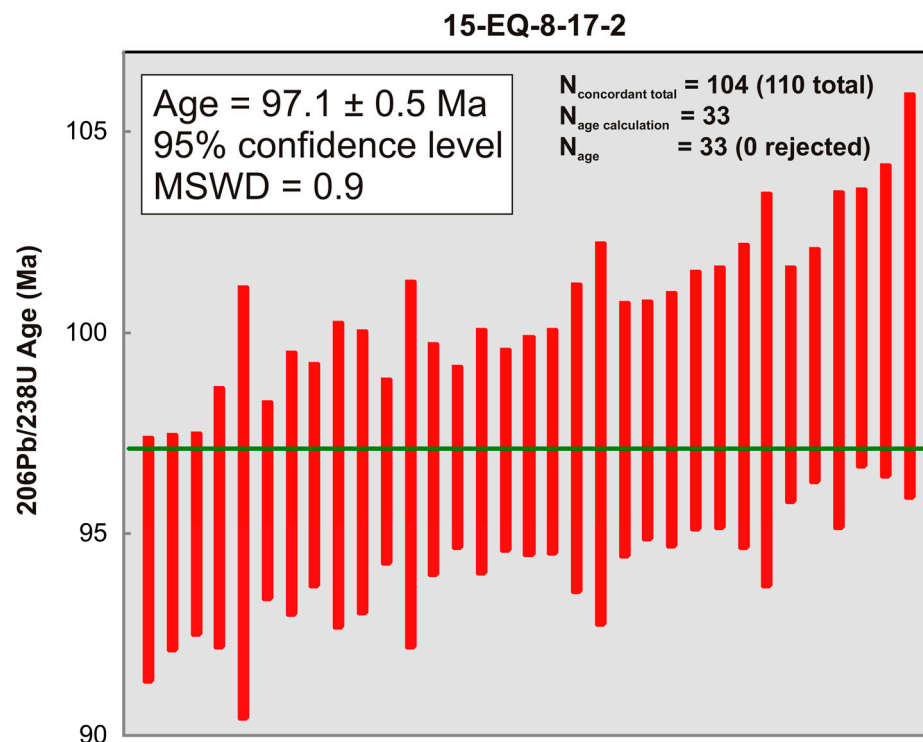


Figure 3. Plot of $^{206}\text{Pb}/^{238}\text{Pb}$ data that yielded an age of 97.1 Ma.

4. Sedimentology

While the Nanushuk Formation encompasses marine and nonmarine facies, this paper focuses primarily on nonmarine fluvial sediments of the rock unit that are exposed along the upper Kukpowruk River (Figure 4). Plant fossils, reflecting successional, riparian, and interfluvial environments (Figure 5A) [12], and upright tree trunks in situ (up to 58 cm diameter) are relatively common in nonmarine facies along the Kukpowruk River.

4.1. Facies Association 1: Thick Sandstone

Medium- to fine-grained sandstones (5–15 m thick) with tabular bedsets, and erosive basal contacts that may contain a basal lag conglomerate, are overlain by sandstones containing large-scale trough cross-beds, and ripple laminations and, less commonly, horizontal laminations. In some cases, sandstones are apparently massive, and they typically fine upwards. Multistory, very fine- to coarse-grained, tabular sandstones up to 10 m thick (Figure 5B) may also be present. These sandstones may be pebbly, although trough crossbedding and ripple cross-lamination typically are present. Siderite intraclasts may be present at the base of sandstones. Lateral accretion surfaces 2–10 m thick may also occur. Sandbodies are typically lenticular but lateral pinch-outs are not always observed, owing to the limited extent of the outcrop. Interbeds of laminated siltstone, mudstone, or coaly shale may be present between sandstone beds.

Two (2 to 5 m thick), very fine- to fine-grained trough cross-bedded and/or ripple cross-laminated sandstones with flat to irregular basal contacts either fine upwards or exhibit no apparent grain size trend. This facies association typically incises into, or grades upward into, interbedded sandstone and mudstone or into mudstones or coal with thin sandstone interbeds. In situ root traces and plant fossils are common.

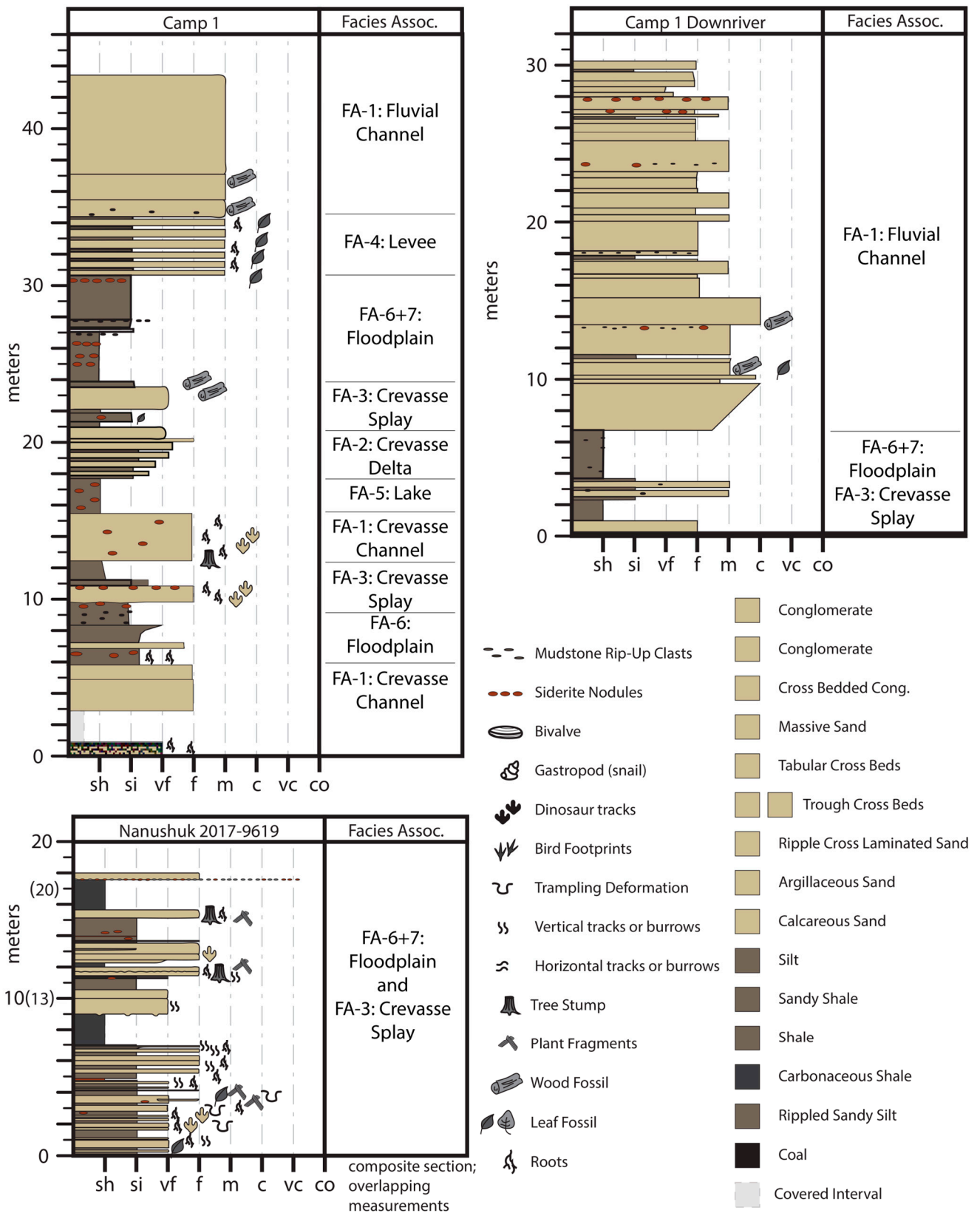


Figure 4. Cont.

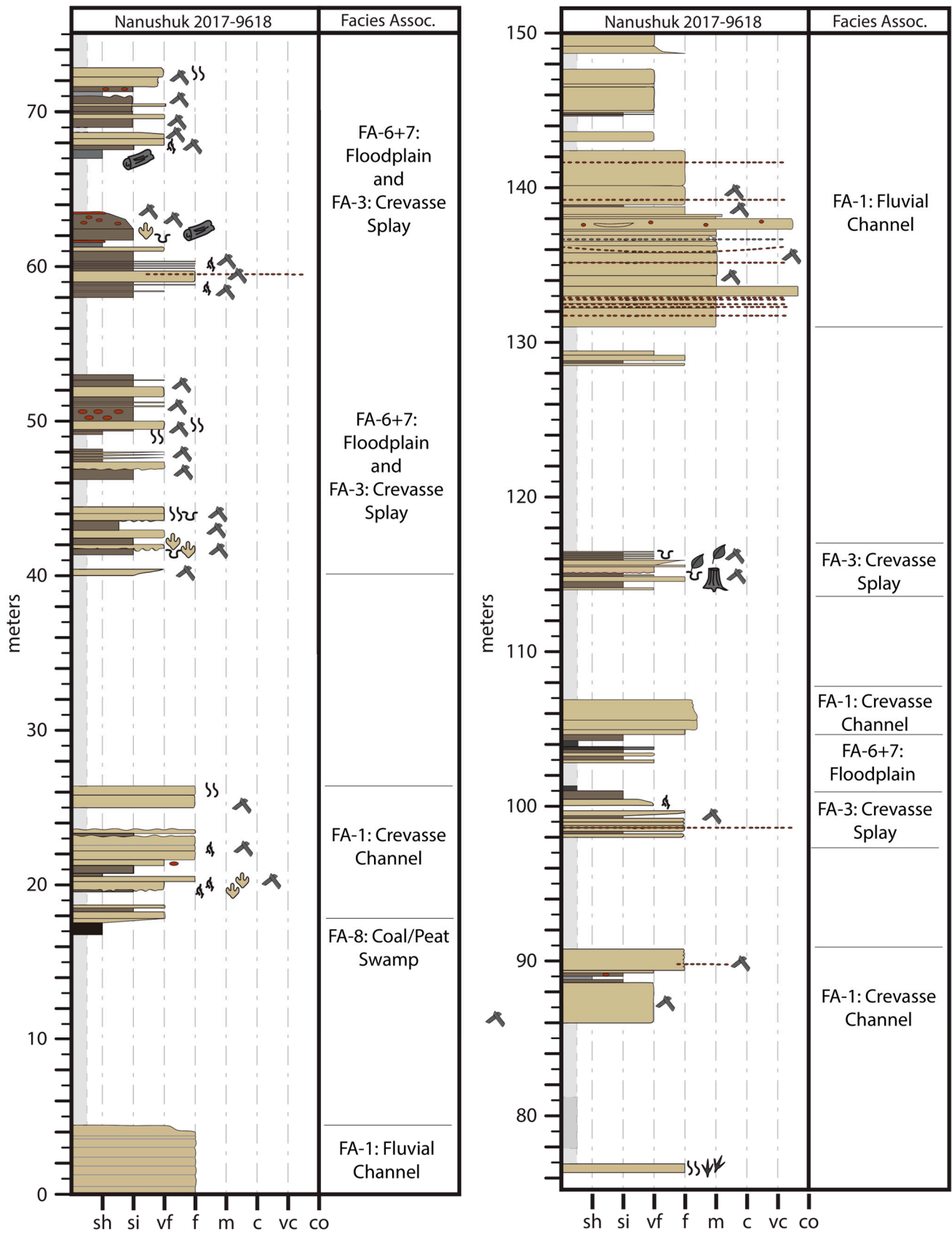


Figure 4. Cont.

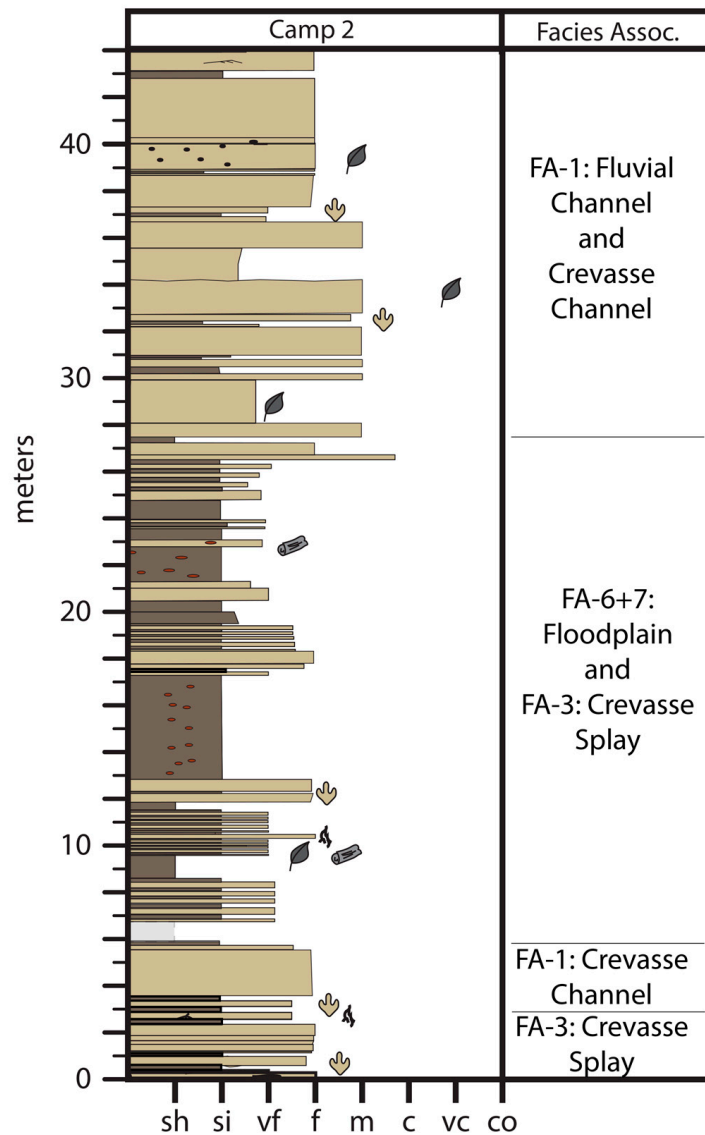


Figure 4. Representative measured sections of fluvial sedimentary successions along the Kukpowruk River, NW Alaska. Legend is shown in lower right. Representative measured sections of fluvial successions along the Kukpowruk River, NW Alaska. See Figure 3 for legend. Representative measured sections of fluvial successions along the Kukpowruk River, NW Alaska. See Figure 3 for legend.

4.2. Interpretation

This facies association is interpreted as fluvial channel deposits representative of large, high sinuosity, mixed-load, meandering channels. Thinner sandstones suggest that smaller, mixed-load, meandering channels, or small crevasse channels were also present. Lateral accretion surfaces indicate that channels migrated laterally across floodplains [39]. Multistory sandstones suggest deposition within a meander belt complex. Mud partings and shale clasts suggest variable flow conditions, and intraformational siderite clasts and mud rip-up clasts suggest that channels were eroding adjacent floodplains. The presence of root traces in the upper layers of some channel sandstones, and the presence of in situ standing tree trunks, indicate that point bars supported vegetation following channel migration, or that some small channel areas were emergent during low flow conditions [40].

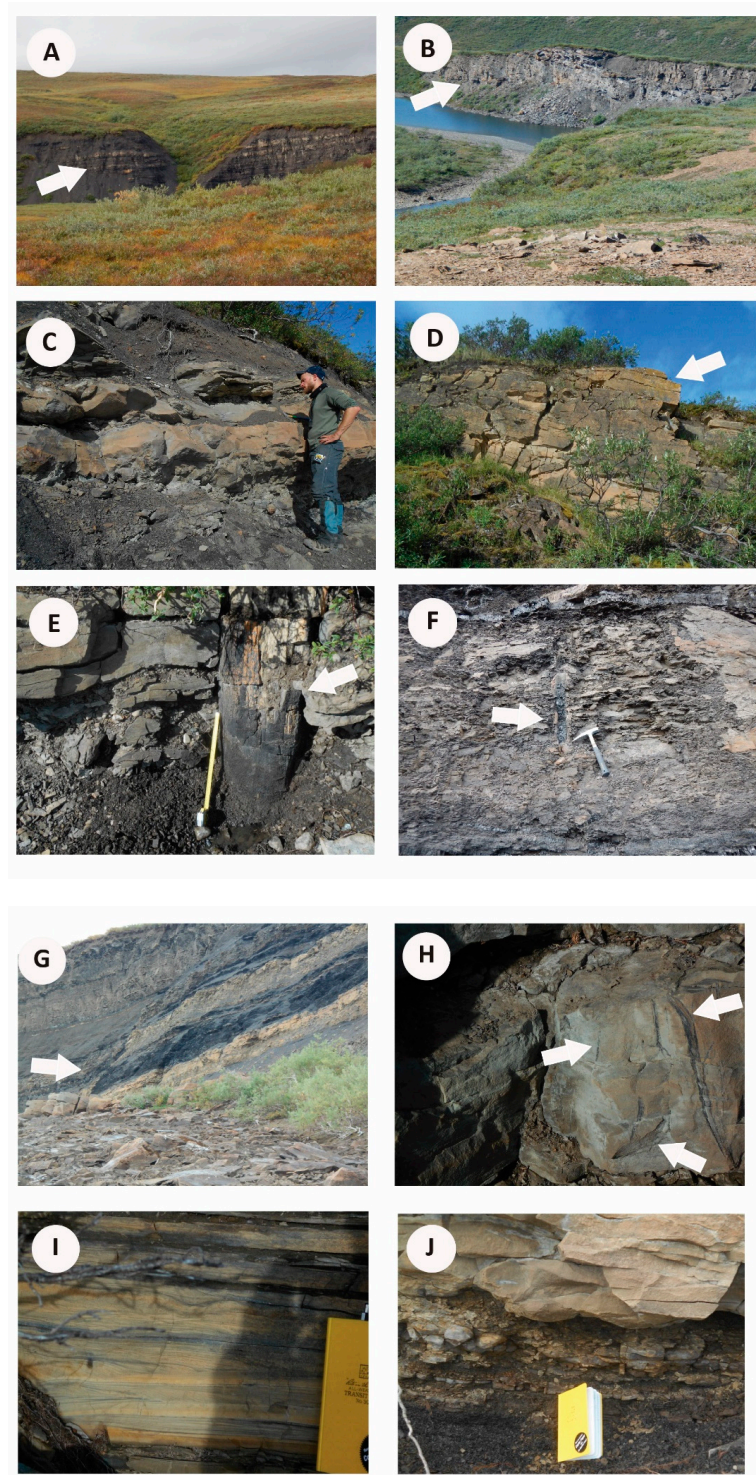


Figure 5. (A) Interbedded sandstone, siltstone, shale, and coal typical of floodplain facies. (B) Multi-story channel-fill sandstone. (C) Floodplain mudstone and sandstone with standing trees at base (not shown). (D) Trough cross-bedded channel sandstone. (E) Standing tree trunk rooted in floodplain mudstone and sandstone (max. 58 cm diameter). (F) Floodplain mudstone with standing tree (adjacent to hammer length = 33 cm). (G) Interbedded, ripple-laminated sandstone, siltstone, shale, and coal typical of a poorly drained floodplain. (H) Large carbonaceous root traces in splay sandstone. (I) Ripple cross-laminated sandstone with abundant organic fragments (coffee grounds) on forests. (J) Floodplain mudstone coarsening upward into splay and levee sandstone sheets.

4.3. Facies Association 2: Interbedded Sandstone and Mudstone

Interbedded, very fine- to fine-grained, lithic sandstone and mudstone (Figure 5C) comprise this facies association. Sharp-based, coarsening-upward intervals of very fine- to fine-grained, ripple cross-laminated sandstone beds with 1–10 cm thick-mudstone interbeds occur. Sandstones thicken upward and they may display horizontal lamination and ripple cross-lamination 1–3 cm thick (Figure 5C). Siltstone interbeds may be ripple cross laminated and typically contain organic fragments, fossils, and coal rip-up clasts. This facies association ranges in thickness from 1 to 3 m, and may be rooted and contain in situ tree trunks up to 30 cm wide.

4.4. Interpretation

Sandier upward successions suggest a change from low energy to higher energy conditions indicating upward shallowing that may result from crevasse delta progradation into a floodplain lake or pond. Ripple cross-laminated interbedded sandstone, siltstone, and mudstone suggest periodic inputs of higher energy unidirectional flows into quiet water. This facies association represents the deposition of a crevasse delta and/or mouth bar [41,42].

4.5. Facies Association 3: Tabular or Lenticular Sharp-Based Sandstone

Very fine to fine sandstones (0.1–2 m thick) without vertical grain size trends comprise this facies association. Individual sandstones may be sharp based, tabular, or lenticular (Figure 5D), and display ripple cross-lamination and trough crossbeds. Plane beds are rare. Individual sandstones typically contain disseminated organic matter. Sandstones are typically rooted and may contain in situ tree trunks and coaly plant fragments (Figure 5E,F). This facies association is typically overlain by siltstones and mudstones.

4.6. Interpretation

Non-channelized flow is suggested by sandstone sheets with sharp bases [43,44]. The grain sizes and bedforms present suggest that bedload was being transported by turbulent flow across floodplains. Small channels within the tabular sandstones suggest a crevasse splay distributary system [45].

4.7. Facies Association 4: Rooted Siltstone and Sandstone

Planar laminated and current ripple cross-laminated fine sandstones (0.1–10 cm thick), with siltstone and/or carbonaceous mudstone interbeds comprising this facies association (Figure 5E). Sandstones coarsen upward. Upper surfaces of sandstones are typically rooted, or they may be rooted throughout, overlain by an organic-rich layer. Basal contacts may be erosional or gradational.

4.8. Interpretation

The sheet-like form of these beds, along with a variety of current-formed structures, suggests non-channelized flow [43,44]. The grain size and bedforms suggest bedload and suspended load were simultaneously deposited. The presence of root traces throughout this facies association suggests that episodic aggradation allowed vegetation to recolonize following deposition. Organic-rich interbeds suggest the presence of organic litter that was buried by subsequent floods. This facies is interpreted to represent levee deposition [42,46].

4.9. Facies Association 5: Platy Mudstone and Siltstone

Dark grey or brown laminated platy mudstone, silty mudstone, or muddy siltstone (0.1–3 m thick) comprise this facies association. Black, brown, and orange color banding may occur. The upper few cm of beds may display ripple cross-laminations. Some intervals have occasional lenses of cm-scale silty sandstone. Mm- to cm-scale siderite nodules are typically observed.

4.10. Interpretation

Laminated or platy siltstone and mudstone suggest deposition under low-energy environments. Dark colors result from organic matter content. Ripple cross-laminations suggest shallow water deposition. The abundance of plant fossils, absence of marine fossils, and association with floodplain mudstones, crevasse splays, and coals suggest deposition in small ponds or lakes on floodplains [46].

4.11. Facies Association 6: Dark Brown to Brownish-Grey, Blocky Mudstone

This facies association consists of blocky structured, medium to dark grey or brownish grey mudstone and muddy siltstone (0.1–10 cm thick). Individual beds contain few, fine orange, and reddish-brown mottles (Figure 5F), as well as mm- to cm-scale carbonaceous root traces. Isolated siderite nodules may be present. Waxy-textured clay coatings may be present on blocky peds. These units typically occur in upward-fining succession or within interbedded sandstone, siltstone, and mudstone units.

4.12. Interpretation

Blocky textures, root traces, and oxidized siderite indicate pedogenic processes within the vadose zone, or in a zone of water table fluctuation. Blocky structure develops as a result of shrinking and swelling of clay particles resulting from alternating wetting and drying [47]. Waxy clay coatings indicate weak clay illuviation, which requires sufficient soil wetting to permit physical washing of colloidal clay through the soil in suspension, followed by sufficient drying out so that the clays are retained on peds [48]. Orange mottling suggests iron translocation under variable to poorly drained conditions. The presence of siderite along with grey-brown colors indicate conditions were well-drained enough to allow decomposition of organics. These features are consistent with pedogenesis on floodplains where water tables fluctuated frequently. Taken together these features suggest weakly developed paleosols that developed under alternating redox conditions on an imperfectly drained floodplain [49,50].

4.13. Facies Association 7: Pale Grey, Sideritic Mudstone

Massive to nodular, pale grey to orange-grey, silty mudstone to very-fine sandstone with carbonaceous roots (1–10 cm long), plant fragments, and siderite nodules (1–15 cm diameter) comprise this facies association. Coaly root traces and fine carbonaceous rootlets typically occur. Well-developed bedding may be disrupted by large siderite nodules that may contain carbonaceous plant fragments within them.

4.14. Interpretation

The pale grey-to-grey coloring, siderite nodules, and plant detritus in this facies association suggest a reducing environment and abundant organic matter [47,48]. Organic matter decomposition is prevented by anaerobic conditions. Weak structure, mottling, and large root traces are indicative of pedogenic development on a poorly drained or hydromorphic floodplain.

4.15. Facies Association 8: Coal

This facies association comprises very dark grey to black fissile to friable coal (0.1–3 m thick) (Figure 5G). Coalified or carbonaceous leaf and twig fragments, root traces (Figure 5H) bark, and fine-grained organic matter are present. Thinner coals containing more clastic material result in low-grade coals or coaly shales. Thin coals may be interbedded with lenticular, ripple cross-laminated, very fine-grained sandstones (Figure 5I) overlying thin mudstone interbeds (Figure 5J). Thicker coals with less clastic material may contain iron oxide mottles or nodules, as well as siderite nodules (up to 5 cm in diameter), and tubules (10–15 cm long).

4.16. Interpretation

Thick coals suggest a wet or waterlogged environment with little clastic input where the organic matter accumulation rate is equal to the subsidence rate. Low clastic contents of thick coals indicate peat swamps were isolated for long periods from deposition on floodplains [51]. Thinner coals with more clastic material may represent accumulations of leaf litter on poorly drained, well-vegetated floodplains.

5. Fossil Vertebrates

A limited record of fossil bone material has been recovered from the Nanushuk Formation, such as a distal ornithopod humerus figured in Fiorillo [52]. In contrast, there is an emerging dinosaurian ichnological record that is diverse, and abundant and will be broadly discussed here.

The track surface scan models for the figures were constructed using Agisoft Metashape Professional Version 1.8.3. The photographs were taken by Nikon D5100 at a resolution of 4928×3264 . The reconstructed models are presented two-dimensionally in orthographic views, occasionally in solid grey models to better illustrate the track topology.

Initial survey work along the Kukpowruk River of the North Slope of Alaska in the summers of 2015–2017 produced approximately 75 isolated discoveries of trace fossils attributable to dinosaurs from fluvial, alluvial, and deltaic settings. Many tracks were found in situ in cross-section, as part of bioturbated horizons in outcrop (Figure 6). Unless features (i.e., distinct toe impressions) were found that helped identify the track makers, these tracks were recorded simply as tracks. When tracks were found in planar view, and showed distinct morphology, those tracks were attributed to large and small theropods, avian theropods, and bipedal and quadrupedal ornithischians. With the possible exception of the quadrupedal ornithischian tracks described below, no ichnotaxonomic group was correlated to any particular depositional setting.



Figure 6. Photograph of bedding plane with an undulating lower contact. These undulations in the fine-grained sandstone are interpreted to be dinosaur footprints in cross-section. Geology hammer for scale (length = 33 cm).

5.1. Non-Avian Theropods Tracks

Tracks attributable to non-avian theropods are uncommon. All the non-avian theropod tracks discovered so far from this region are tridactyl and lack hallux impression. The digits of these tracks are long and thin, and they taper to a point (Figure 7). In addition to the sharply terminated distal ends, in some examples, digit III also has a slight sinusoidal curve (Figure 7). The lengths of these tracks range from 16–27 cm long, while the widths range from 13–22 cm. The morphology of these tracks allows attribution of the track-maker as a medium to a large non-avian theropod. For the maximum track length (27 cm),

using an equation of $4 \times$ the track length as an estimate of hip height, and $3.75 \times$ the hip height as an estimate of body length [53–55], this track was made by a non-avian theropod approximately 4 m long. Given the incomplete nature of the fossil record, time correlative comparisons within North America are challenging. Where the skeletal remains are more complete, this estimated body size is much smaller than the Cenomanian North African theropod, *Carcharodontosaurus* [56], but within the size range of somewhat younger Turonian theropods such as the North American *Suskityrannus* [57] and the Asian *Timurlengia* [58]. Likewise, the length of the smallest track (16 cm) suggests a body length of approximately 2.5 m.

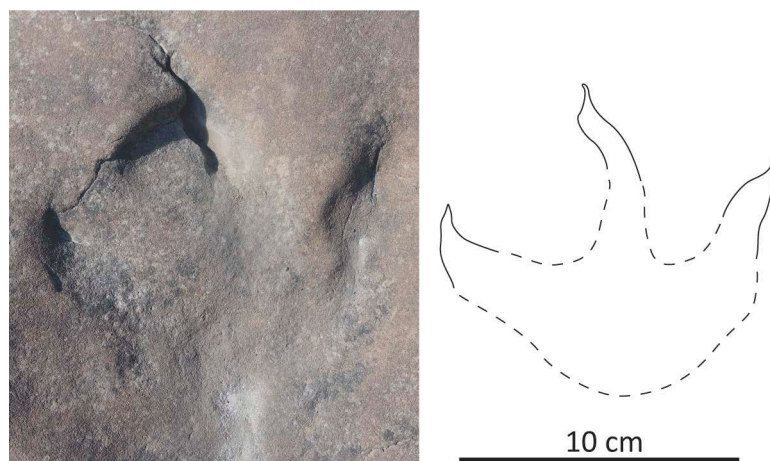


Figure 7. Theropod track (field number 16AF8-12-3). Note the sinusoidal curve of the middle toe impression. Scale bar equals 10 cm.

5.2. Avian Theropod Tracks

In this study, tracks attributable to fossil birds represent two of the broad categories assigned to modern bird tracks [59,60]: anisodactyl and incumbent anisodactyl. The arrangement of digits in anisodactyl tracks has three toes (digits II–IV) that point forward and one toe (digit I) that points backward. Though very similar in morphology, incumbent anisodactyl tracks also have digits II–IV that point forward but have a greatly reduced or non-existent impression left by digit I. This suggests that digit I is greatly reduced or non-existent. Tracks with full webbing between digits II–IV are palmate tracks, and within palmate tracks, the impression left by digit I is greatly reduced or non-existent. Thus, palmate tracks can resemble incumbent anisodactyl tracks. But the former group of tracks also differs from the latter in that digits II and IV are somewhat curved medially. Rezendes [59] and Elbroch and Marks [60] point out that morphological variation within modern tracks of known trackmakers can result from variability in sediment texture, consistency, and moisture, thereby yielding tracks that belong to more than one morphological group. Variance in morphology due to the transmission of significant pressure into sediment sublayers seems unlikely given the small nature of these avian tracks.

The most abundant avian theropod tracks are small with three slender toe impressions (Figure 8). The individual pes impressions are typically wider than long, though some are approximately as wide as long. Lengths within all tracks found range from 3.1 to 6.9 cm, though the majority are approximately 4 cm long. Similarly, widths within all tracks were found to range from 4.1 to 7.1 cm, while most tracks have an approximate 5 cm in width. Hallux (digit I) impressions are absent, though two tracks (Figure 9) have a suggestion of hallux. Those without a hallux impression can be attributed to the ichnogenus *Aquatilavipes*. Digit III for these tracks is the longest and digit IV is approximately the same length as digit II. The morphology of this fossil track compares well with the *Aquatilavipes swiboldae* from the Aptian of British Columbia [61]. The tracks with a suggestion of a hallux are tentatively assigned the ichnogenus *Ignotornis*, though the webbing that can be associated with this

ichnogenus [62] was not observed. Both ichnotaxa have been reported in several rock units in western North America, as well as Asia [61–65].



Figure 8. Small tridactyl tracks with three slender toe impressions attributable to avian theropods. The heat map (right) signifies red for higher elevations and blue for lower elevations. The scale bar is in centimeters.

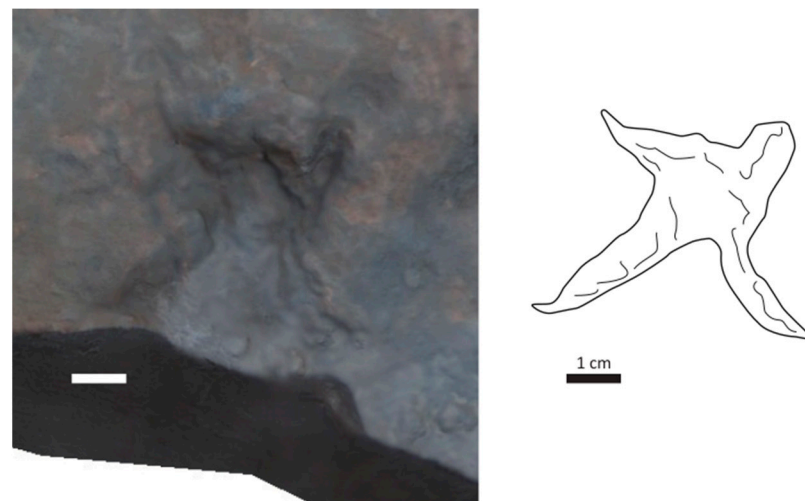


Figure 9. Small tridactyl track with three slender toe impressions and the suggestion of a hallux. This track is attributed to the avian theropods, *Ignatornis*. Scale bar represents one centimeter.

5.3. Ornithischian Tracks

The most abundant tracks can be attributed to ornithischian pedal tracks. This attribution is based on the overall morphology of three short, wide, ovoid digit impressions, and an associated large, rounded heel (Figure 10). Individual tracks are wider than long, with the width ranging from 15 to 39 cm and the length ranging between 12 and 31 cm. No evidence of a bi-lobed heel was observed, a defining characteristic of tracks attributed to hadrosaurs and specifically the ichnogenus *Hadrosauropodus* [66–68]. Rather, the large, rounded heel and short, broad digits are characters allowing attribution to the ichnotaxon *Caririchnium* [69]. Similar to much of the lower latitude Cretaceous Western Interior Seaway margin deposits, isolated tracks of large ornithopods are the most encountered dinosaurian ichnites in Upper Cretaceous high-latitude deposits of North America [67,68,70–72], and

that pattern holds for the older Nanushuk Formation along the Kukpowruk River. Though it is worth noting that, compared to the lower latitude Cenomanian records of *Caririchnium*, the Nanushuk tracks discussed here tend to be smaller on average (Woodbine Formation: 38.8–46.6 cm in length [73]; Tongfosi Formation: 33.6–50 cm in length, [74]), it is unclear if this pattern has taxonomic or environmental implications, or perhaps some other unrecognized significance.

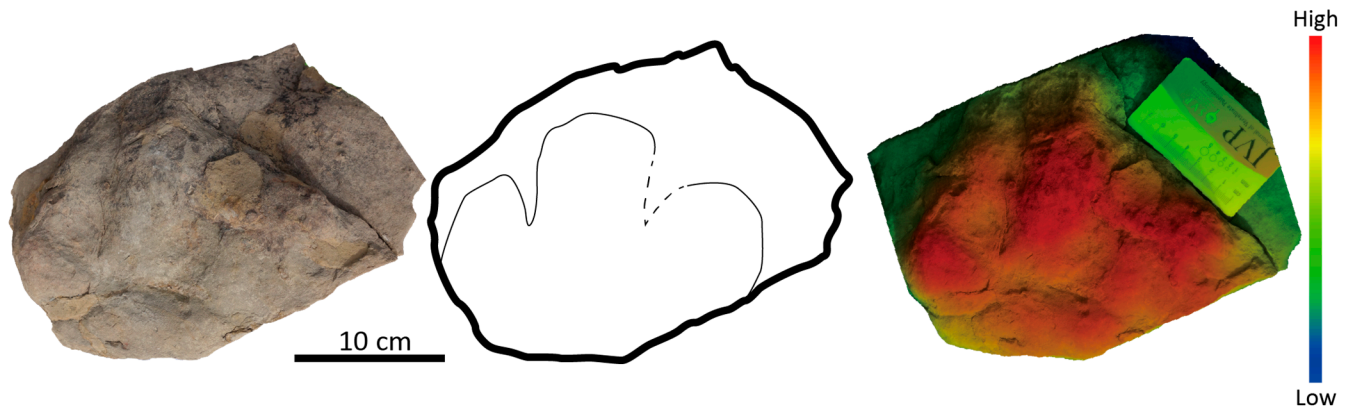


Figure 10. Large track with a rounded heel, and short, broad digits attributable to the ichnotaxon, *Caririchnium*, a bipedal ornithischian. The heat map (right) signifies blue for higher elevations and green for lower elevations. Scale bar represents ten centimeters.

The morphology of ceratopsian and thyreophoran feet is very similar and differentiating the two can be challenging. McCrea et al. [75] examined the skeletal and footprint characters distinguishing ankylosaur tracks from ceratopsian tracks, and those characters are summarized in Table 1. Their study pointed out a significant difference between the two groups of dinosaurs in that ankylosaurs had proportionately longer toes when compared to metatarsals, while in ceratopsians the relationship is reversed, with metatarsals longer than the toes. Thus, thyreophoran tracks have well-developed toe impressions when compared to ceratopsians. Further, in ankylosaur manus prints, the distribution of digit impressions is arcuate, resulting in a star-shaped track. Within the track assemblage found along the Kukpowruk River, there are several examples of tracks attributable to quadrupedal ornithischian dinosaurs.

Table 1. List of characters that distinguish ceratopsian tracks from ankylosaur tracks. Table combines skeletal characters and footprint characters. Characters taken from McCrea et al. [75].

Ankylosaur Skeletal	Ceratopsian Skeletal
<ul style="list-style-type: none"> - 4 digits on pes - 5 digits on manus - manual digit V reduced - longer toes compared to metatarsals 	<ul style="list-style-type: none"> - 4 digits on pes - 5 digits on manus - manual digits IV and V reduced - shorter toes compared to metatarsals - digits have appearance of tapering distally
Ankylosaur Footprint	Ceratopsian Footprint
<p>(<i>Tetrapodosaurus</i> ichnosp.)</p> <ul style="list-style-type: none"> - longer toe impressions - digit I most prominent 	<p>(<i>Ceratopsipes</i> ichnosp.)</p> <ul style="list-style-type: none"> - symmetrical appearance - digit I not the most prominent

The first pattern observed in tracks found in exposures along the Kukpowruk River is that of very short, rounded toes on a nearly symmetrical track, without one digit being prominent (Figure 11). The tracks of quadrupedal ornithischians discussed here are

attributed to the ceratopsian ichnogenus *Ceratopsipes*, though we recognize that somewhat older ceratopsians, such as *Aquilops* and *Auroraceratops*, were bipedal and lightly built, and possibly left tracks with a different morphology. Further, it should be noted that the track shown in Figure 10 is rather large for an *Auroraceratops*-sized animal; thus, this larger potential ceratopsian might have already switched to a more quadrupedal position.

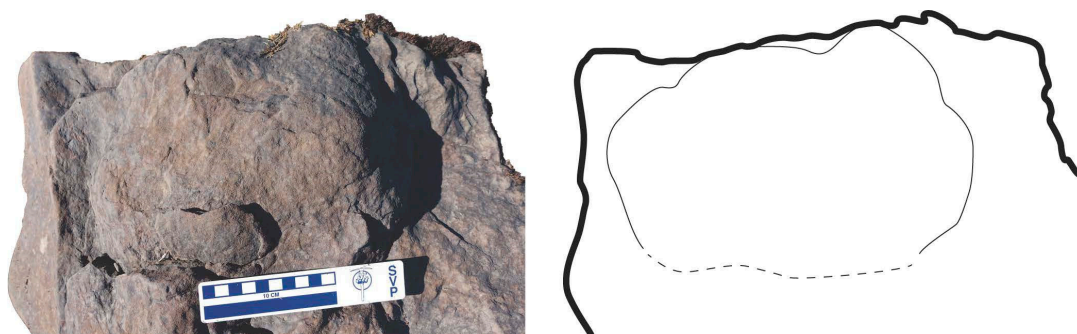


Figure 11. Very short, rounded toes on a nearly symmetrical track, without one digit being prominent attributed to the ichnogenus, *Ceratopsipes*, considered to be a quadrupedal ornithischian. Scale bar is in centimeters.

The second pattern observed in tracks attributable to quadrupedal ornithischians are tracks that are more star shaped, with defined digits (Figure 12). The track in Figure 11 is a five-toed manual track whose finger impressions are well separated from each other. The track is approximately 15 cm wide and 10 cm long. The first and fifth phalanx impressions are angled more than 180 degrees as in the *Tetrapodosaurus borealis* holotype (NMC 8556) from the Aptian–Albian Gething Formation [75], which is now widely accepted to belong to Ankylosauria [76].

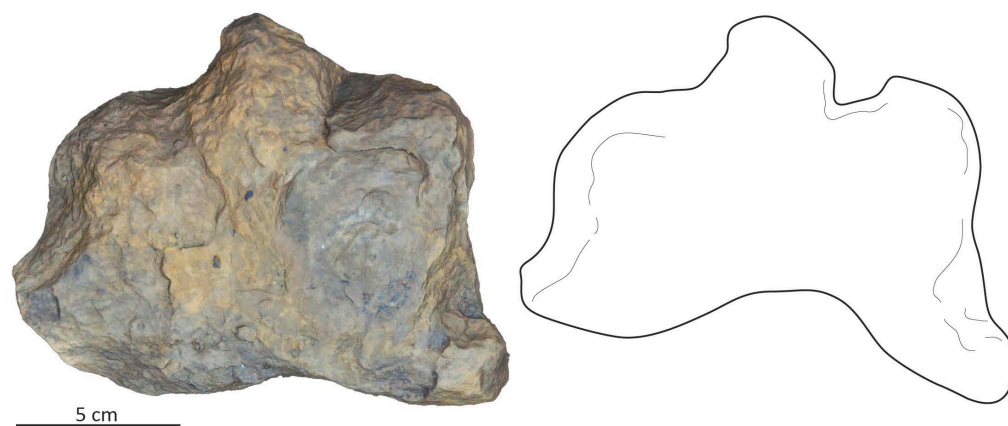


Figure 12. Star-shaped track with defined digits attributable to the ichnogenus, *Tetrapodosaurus*, considered to be a quadrupedal ornithischian. The scale bar represents five centimeters.

The *Tetrapodosaurus* track is the northernmost ankylosaur occurrence known today. Previously, Gangloff [77] reported a partial skull of a nodosaurid ankylosaur *Edmontonia* sp. from the upper Campanian–lower Maastrichtian Matanuska Formation exposed along the Caribou Creek in Talkeetna Mountains, Alaska. Godefroit et al. [78] also reported an isolated ankylosaur tooth from the Maastrichtian Kakanaut Formation, Russia. The new fossil record reported herein extends ankylosaur biogeography further north and in much older dates. While the Nanushuk Formation *Tetrapodosaurus* is much older than the Matanuska Formation nodosaurid, nodosaurids are widely known from the northern hemisphere including North America (e.g., *Sauropelta*), Europe (e.g., *Europelta*), and Asia (e.g., *Dongyangopelta*) during this time range. Of these two ichnogenera, *Ceratopsides* and

Tetrapodosaurus, the latter is approximately twice as frequent as the former in the more nonmarine facies studied in this report.

6. Paleoclimate

An inverse relationship between mean annual precipitation (MAP) and the carbon isotope value of plant tissue (specifically leaves) of C3 plants is documented by Kohn [79] and Diefendorf et al. [80]. While leaves were not recovered from these localities, coalified wood fragments were abundant and analyzed for their stable carbon isotope values. Samples were homogenized and treated with 0.5 M HCl to remove any carbonate mineral. Samples were then rinsed, dried, and rehomogenized. Carbon isotope values were determined via combustion on a Costech 4010 Elemental analyzer coupled to a ThermoFinnigan Delta + XP at the University of Texas at San Antonio. Analyses were corrected to VPDB using internal and international standards (USGS 24, ANU Sucrose (IAEA-C6), and IAEA 600). Reproducibility is monitored via the repeated analyses of Peach Leaves (NIST 1547) and Dogfish muscle (DORM) and is reported as $\pm 0.2\%$.

For this study, we utilize the following equations to determine MAP:

$$\Delta_{leaf} = 5.54 (\pm 0.22) * \log_{10}(MAP) + 4.07 (\pm 0.70) \quad (1)$$

$$\Delta_{leaf} = \frac{\delta^{13}C_{atm} - \delta^{13}C_{leaf}}{1 + \delta^{13}C_{leaf}/1000} \quad (2)$$

The $\delta^{13}C_{leaf}$ value was determined by applying a -1% correction to the wood carbon isotope value [81]. It is not expected that the coalification process would alter the $\delta^{13}C$ values of plants [82]. Barral et al. [83] provide values for the $\delta^{13}C$ values of the atmosphere by stage for the Cretaceous period. We utilize -5.97 for $\delta^{13}C_{atm}$ for the calculation of Δ_{leaf} . Equation 1 [80] was then utilized to determine mean annual precipitation.

The $\delta^{13}C$ values for wood fragments range from -27.0% to -25.8% (Table 2). Using Equation (1) [80], MAP ranges from 1334 mm/year to 2284 mm/year. These preliminary estimates are greater than modeled precipitation rates (218 to 642 mm/year [84]; 150 to 963 mm/year [85]), emphasizing the fact that climate model and climate proxy estimates in polar regions still require reconciliation. The average MAP for our samples yields an estimate of 1770 mm per year.

Table 2. The $\delta^{13}C$ values for wood fragments collected from the Nanushuk Formation along the Kukpowruk River during this project.

Sample Name	$\delta^{13}C$ ‰ vs. VPDB	$\delta^{13}C_{leaf}$ ‰ vs. VPDB	Δ_{leaf}	Mean Annual Precipitation (mm/year)
KUKP-1	-26.6	-27.7	22.2	1901
KUKP-3	-27.0	-28.0	22.7	2284
KUKP-4	-25.8	-26.8	21.4	1334
KUKP-5	-26.1	-27.1	21.8	1562

7. Discussion

In contrast to the study of Cretaceous Alaskan dinosaurs of the Campanian–Maastrichtian, the documentation of fossil vertebrates from older Cretaceous rocks has been limited [28,52,86–88]. In the mid-1980s, dinosaurian fossil skin impressions and footprints were reported from the Cretaceous of northwestern Alaska in what is now recognized as the Nanushuk Formation [87]. Despite not being described in detail, the figures provided by the authors suggested that these traces can be attributed to ornithopods. Additional three-toed tracks in the Nanushuk Fm. have been photographed and presented as sedimentologic oddities elsewhere in the literature [21], while a four-toed track attributed to a neoceratopsian

has also been reported from this rock unit [11]. Though the record of fossil bones from the Nanushuk Formation is far from robust, the dinosaur bones found thus far can be attributed to members of the Ornithopoda [52]. This current work has shown a remarkable undocumented dinosaur ichnological record, which has been under-appreciated by previous geologists working in this rock unit and allows for integration with the detailed paleobotanical study along the same river by Spicer and Herman [12]. Further, the new isotopic date for at least part of the section discussed here is consistent with other ash dates published for nonmarine facies within the Nanushuk Formation elsewhere [89], not only suggesting that our conclusions are constrained within the Cenomanian but that much of the nonmarine section for this rock unit is of this age.

In their detailed study, Spicer and Herman [12] noted consistent patterns between depositional environments and plant associations. These plant communities ranged from a marginal marine and early successional marsh/heath community dominated by horsetails (*Equisetum*) and ferns, to shrubby to forested river margin communities, and mire forest communities. While this resolution in plant communities is intriguing, the same community resolution is not readily apparent from the vertebrate ichnological record along the Kukpowruk River in this study. Our documentation shows no comparably clear pattern. There is only a slight suggestion with the tracks recorded in this study that the *Ceratopsipes*/*Tetrapodus* track makers may have been restricted to the more nonmarine part of the stratigraphic section exposed along this river. This is in contrast with the association of *Tetrapodus* tracks with coastal deposits in younger Cretaceous deposits in the ancient high latitudes [90].

Figure 13 shows the relative abundances of four broad ichnotaxonomic groups of tracks found along the Kukpowruk River. Of note is the dominance of tracks attributable to bipedal ornithischian dinosaurs. This is in contrast to the correlative Dunvegan Formation of nearby northeast British Columbia where the tracks of *Tetrapodus* dominate the vertebrate ichnology record [91]. To explain this abundance of *Tetrapodus* tracks in the Dunvegan Formation, it has been suggested that this may be tied to the diversity and abundance of angiosperms found in the rock unit [92]. The diversity of floral communities within the Nanushuk Formation along the Kukpowruk River where angiosperms were only a minor component of the floral landscape [12] suggests such a landscape favored bipedal ornithischians.

Also of note within the dinosaur ichnofauna is that approximately 15% of the record (Figure 13) is represented by fossil bird tracks, specifically shorebird-like tracks (e.g., *Aquatilavipes*). This unexpected abundance of bird tracks in the ancient Arctic is intriguing. Nearly half of extant shorebirds that reside in North America take advantage of the high seasonal productivity of the warm months to breed in the modern Arctic [93]. The high frequency of fossil bird tracks along the Kukpowruk River may suggest that the effects of seasonal ecosystem productivity were a similar driver for ancient vertebrate productivity and biodiversity within this group of fossil animals.

Finally, tectonic reconstructions suggest that the formation of the land bridge connection between Asia and North America occurred by the Albian [94] and was used by neoceratopsians at this time [11]. The track diversity shown in this study demonstrates some level of more advanced ecological complexity by vertebrates regarding niche separation and resource use just a few million years later.

The MAP data presented here show wetter conditions than conditions recorded in later Cretaceous environments at comparable latitudes [6]. A warmer wetter Arctic in the Cenomanian is consistent with other climate models/data and these tracks show that the wetter conditions would have allowed a suitable environment for all these dinosaurs. This study provides a framework for further paleoecological and paleoclimatic analyses in the terrestrial Cretaceous Arctic during this important window of greenhouse conditions.

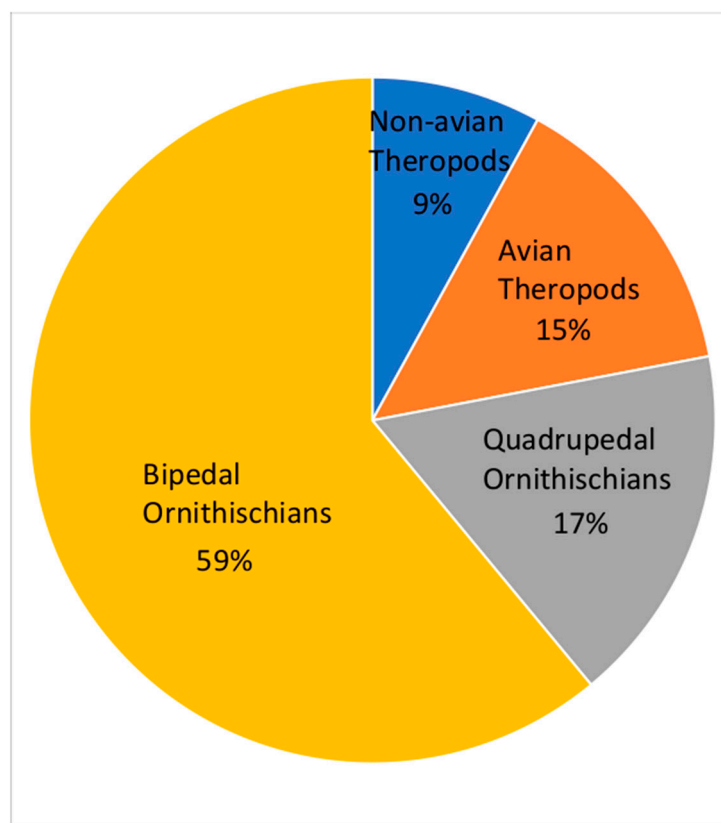


Figure 13. Pie diagram showing the relative abundances of four broad groups of ichnotaxa found in this study. Note the assemblage is dominated by the occurrence of bipedal ornithopods; also note the abundance of avian theropod (bird) tracks.

8. Conclusions

The Nanushuk Formation was deposited at high latitude in the mid-Cretaceous greenhouse Arctic, and records deposition on marginal marine, lower delta plain, and upper delta plain environments. The upper delta plain, exposed along the Kukpowruk River, is dominated by a meandering fluvial system, including floodplains, crevasse channels and splays, levees, and peat swamps. Radiometric data indicate that the rocks representing these environments are Cenomanian in age. The Nanushuk Formation contains abundant evidence of thriving vegetational communities. There is evidence of a diverse fauna consisting of both avian (birds) and non-avian theropods, and quadrupedal and bipedal ornithischians. The environments preserved within the Nanushuk Formation had a MAP averaging 1770 mm per year. This pattern of increased precipitation in the Nanushuk Formation during the Cenomanian is regionally consistent with the global pattern associated with the Cretaceous Thermal Maximum and provides additional evidence of a thriving high-latitude ecosystem during the mid-Cretaceous greenhouse in paleo-Arctic Alaska.

Author Contributions: A.R.F. and P.J.M. designed and conceived the research. A.R.F., P.J.M., G.S., R.T., T.C., Y.K. and E.O. collected field samples and additional data. M.B.S. analyzed the geochemical samples from the Nanushuk Formation. P.O. analyzed the ash sample for this study. All authors contributed to the interpretation, discussion, and writing of the results. All authors have read and agreed to the published version of the manuscript.

Funding: The Explorers Club World Exploration Challenge grant and Friends of ISEM Paleo provided funding to ARF for field work associated with this project.

Data Availability Statement: Data are resposited within each respective institution.

Acknowledgments: We thank Rory Leahy and Carla Tomsich for general assistance in the field.

Conflicts of Interest: The authors declare no conflict of interest.

References

1. Barnosky, A.D.; Hadly, E.A.; Gonzalez, P.; Head, J.; Polly, P.D.; Lawing, A.M.; Eronen, J.T.; Ackerly, D.D.; Alex, K.; Biber, E.; et al. Merging paleobiology with conservation biology to guide the future of terrestrial ecosystems. *Science* **2017**, *355*, eaah4787. [CrossRef]
2. Nogués-Bravo, D.; Rodríguez-Sánchez, F.; Orsini, L.; de Boer, E.; Jansson, R.; Morlon, H.; Fordham, D.A.; Jackson, S.T. Cracking the code of biodiversity responses to past climate change. *Trends Ecol. Evol.* **2018**, *33*, 765–776. [CrossRef]
3. Williams, J.W.; Ordonez, A.; Svenning, J.C. A unifying framework for studying and managing climate-driven rates of ecological change. *Nat. Ecol. Evol.* **2021**, *5*, 17–26. [CrossRef] [PubMed]
4. Kiessling, W.; Smith, J.A.; Raja, N.B. Improving the relevance of paleontology to climate change policy. *Proc. Natl. Acad. Sci. USA* **2023**, *120*, e2201926119. [CrossRef]
5. Parrish, J.T.; Spicer, R.A. Late Cretaceous terrestrial vegetation: A near-polar temperature curve. *Geology* **1988**, *16*, 22–25. [CrossRef]
6. Fiorillo, A.R.; McCarthy, P.J.; Kobayashi, Y.; Suarez, M.B. Cretaceous dinosaurs across Alaska show the role of paleoclimate in structuring ancient large-herbivore populations. *Geosciences* **2022**, *12*, 161. [CrossRef]
7. Hedges, S.B.; Parker, P.H.; Sibley, C.G.; Kumar, S. Continental breakup and the ordinal diversification of birds and mammals. *Nature* **1996**, *381*, 226–229. [CrossRef] [PubMed]
8. Dilcher, D. Toward a new synthesis: Major evolutionary trends in the angiosperm fossil record. *Proc. Natl. Acad. Sci. USA* **2000**, *97*, 7030–7036. [CrossRef] [PubMed]
9. Lloyd, G.T.; Davis, K.E.; Pisani, D.; Tarver, J.E.; Ruta, M.; Sakamoto, M.; Hone, D.W.; Jennings, R.; Benton, M.J. Dinosaurs and the Cretaceous terrestrial revolution. *Proc. R. Soc. B: Biol. Sci.* **2008**, *275*, 2483–2490. [CrossRef] [PubMed]
10. Scott, R.W.; Oboh-Ikuenobe, F.E.; Benson, D.G., Jr.; Holbrook, J.M.; Alnahwi, A. Cenomanian-Turonian flooding cycles: US Gulf Coast and western interior. *Cretac. Res.* **2018**, *89*, 191–210. [CrossRef]
11. Fiorillo, A.R.; Decker, P.L.; LePain, D.L.; Wartes, M.; McCarthy, P.J. A probable neoceratopsian manus track from the Nanushuk Formation (Albian, northern Alaska). *J. Iber. Geol.* **2010**, *36*, 165–174. [CrossRef]
12. Spicer, R.A.; Herman, A.B. The Albian–Cenomanian flora of the Kukpowruk River, western North Slope, Alaska: Stratigraphy, palaeofloristics, and plant communities. *Cretac. Res.* **2001**, *22*, 1–40. [CrossRef]
13. Moore, T.E.; Wallace, W.K.; Bird, K.J.; Karl, S.M.; Mull, C.G.; Dillon, T.T. *The Geology of North America, v. G-1, the Geology of Alaska*; Plafker, G., Berg, H.C., Eds.; Geological Society of America: Boulder, CO, USA, 1994; pp. 49–140.
14. Bird, K.J.; Molenaar, C.M. The North Slope Foreland Basin, Alaska: Chapter 13. *Am. Assoc. Pet. Geol. Mem.* **1992**, *55*, 363–393.
15. Molenaar, C.M. Subsurface correlations and depositional history of the Nanushuk Group and related strata, North Slope, Alaska. In *Geology of the Nanushuk Group and Related Rocks*; U.S. Geological Survey Bulletin: North Slope, AK, USA, 1985; Volume 1614, pp. 37–59.
16. Molenaar, C.M. Depositional history and seismic stratigraphy of Lower Cretaceous rocks in the National Petroleum Reserve in Alaska and adjacent areas. In *U.S. Geological Survey Professional Paper*; U.S. Geological Survey Bulletin: North Slope, AK, USA, 1988; Volume 1399, pp. 593–621.
17. Finzel, E.S.; McCarthy, P.J. *Architectural Analysis of Fluvial Conglomerate in the Nanushuk Formation, Brooks Range Foothills, Alaska*; Alaska Division of Geological & Geophysical Surveys: Fairbanks, AK, USA, 2005; pp. 1–20.
18. Fisher, W.I.; Brown, L.F., Jr.; Scott, A.J.; McGowen, J.H. *Delta Systems in the Exploration for Oil and Gas*; Texas Bureau of Economic Geology: Austin, TX, USA, 1969; pp. 1–78.
19. Huffman, A.C., Jr. *Geology of the Nanushuk Group and Related Rocks*; U.S. Geological Survey Bulletin: North Slope, AK, USA, 1985; Volume 1614, pp. 1–6.
20. Huffman, A.C., Jr.; Ahlbrandt, T.S.; Bartsch-Winkler, S. Geology and exploration of the National Petroleum Reserve in Alaska, 1974 to 1982. In *U.S. Geological Survey Professional Paper*; U.S. Geological Survey Bulletin: North Slope, AK, USA, 1988; Volume 1399, pp. 281–298.
21. Ahlbrandt, T.S.; Huffman, A.C.; Fox, J.E.; Pasternack, I. *Depositional Framework and Reservoir-Quality Studies of Selected Nanushuk Group outcrops, North Slope, Alaska*; U.S. Geological Survey Circular: North Slope, AK, USA, 1979; Volume 794, pp. 14–31.
22. LePain, D.L.; McCarthy, P.J.; Kirkham, R. *Sedimentology and sequence stratigraphy of the middle Albian–Cenomanian Nanushuk Formation in outcrop, central North Slope, Alaska*. Alaska Division of Geological & Geophysical Surveys. *Rep. Investig.* **2009**, *2009*, 1–86.
23. McCarthy, P.J. *Alluvial Facies and Paleosols in the Cretaceous Nanushuk Formation, Kanayut River, North Slope, Alaska: Preliminary Results from the 2001 Field Season*; Alaska Division of Geological & Geophysical Surveys: North Slope, AK, USA, 2003; Volume 1–19.
24. Mull, C.G.; Houseknecht, D.W.; Bird, K.J. Revised Cretaceous and Tertiary stratigraphic nomenclature in the Colville Basin, northern Alaska. In *U.S. Geological Survey Professional Paper*; U.S. Geological Survey Bulletin: North Slope, AK, USA, 2003; Volume 1673, pp. 1–51. Available online: <https://pubs.usgs.gov/pp/p1673/text.html> (accessed on 5 May 2023).
25. Dettnerman, R.L.; Bickel, R.S.; Gryc, G. Geology of the Chandler River region, Alaska. In *U.S. Geological Survey Professional Paper*; U.S. Geological Survey Bulletin: North Slope, AK, USA, 1963; Volume 303-E, pp. 233–324.

26. Shimer, G.T.; McCarthy, P.J.; Hanks, C.L. Sedimentology, stratigraphy, and reservoir properties of an unconventional, shallow, frozen petroleum reservoir in the Cretaceous Nanushuk Formation at Umiat field, North Slope, Alaska. *Am. Assoc. Pet. Geol. Bull.* **2014**, *98*, 631–661. [[CrossRef](#)]
27. Mull, C.G.; Harris, E.E.; Reifentstahl, R.R.; Moore, T.E. Alaska Division of Geological & Geophysical Surveys Report of Investigations. 2000, 2000–2002, 1 sheet, scale 1:63,360. Available online: <https://pubs.usgs.gov/pp/pp1662/biblio.pdf> (accessed on 12 April 2023).
28. LePain, D.L.; Decker, P.L. Lithofacies analysis of the Wainwright #1 continuous core, western Arctic Slope, Alaska: Transition from lower to upper delta plain environments in the Albian–Cenomanian Nanushuk Formation. In *Alaska Division of Geological & Geophysical Surveys Report of Investigation*; Alaska Division of Geological & Geophysical Surveys: North Slope, AK, USA, 2016; Volume 3, pp. 1–56. [[CrossRef](#)]
29. Spicer, R.A. *The Cretaceous World*; Skelton, P., Ed.; Cambridge University Press: Cambridge, UK, 2003; pp. 85–162.
30. Gehrels, G. Detrital Zircon U-Pb Geochronology Applied to Tectonics. *Annu. Rev. Earth Planet. Sci.* **2014**, *42*, 127–149. [[CrossRef](#)]
31. Sundell, K.E.; Gehrels, G.E.; Pecha, M.E. Rapid U-Pb geochronology by laser ablation multi-collector ICP-MS. *Geostand. Geoanal. Res.* **2021**, *45*, 37–57. [[CrossRef](#)]
32. Garza, H.K.; Catlos, E.J.; Chamberlain, K.R.; Suarez, S.E.; Brookfield, M.E.; Stockli, D.F.; Batchelor, R.A. How old is the Ordovician–Silurian boundary at Dob’s Linn, Scotland? Integrating LA-ICP-MS and CA-ID-TIMS U-Pb zircon dates. *Geol. Mag.* **2023**, *160*, 1775–1789. [[CrossRef](#)]
33. Bowring, S.A.; Schmitz, M.D. High-precision U-Pb zircon geochronology and the stratigraphic record. *Rev. Mineral. Geochem.* **2003**, *53*, 305–326. [[CrossRef](#)]
34. Tian, H.; Fan, M.; Valencia, V.A.; Chamberlain, K.; Waite, L.; Stern, R.J.; Loocke, M. Rapid early Permian tectonic reorganization of Laurentia’s plate margins: Evidence from volcanic tuffs in the Permian Basin, USA. *Gondwana Res.* **2022**, *111*, 76–94. [[CrossRef](#)]
35. Coutts, D.S.; Matthews, W.A.; Hubbard, S.M. Assessment of widely used methods to derive depositional ages from detrital zircon populations. *Geosci. Front.* **2019**, *10*, 1421–1435. [[CrossRef](#)]
36. Herriott, T.M.; Crowley, J.L.; Schmitz, M.D.; Wartes, M.A.; Gillis, R.J. Exploring the law of detrital zircon: LA-ICP-MS and CA-TIMS geochronology of Jurassic forearc strata, Cook Inlet, Alaska, USA. *Geology* **2019**, *47*, 1044–1048. [[CrossRef](#)]
37. Trop, J.M.; Benowitz, J.; Cole, R.B.; O’Sullivan, P. Cretaceous to Miocene magmatism, sedimentation, and exhumation within the Alaska Range suture zone: A polyphase reactivated terrane boundary. *Geosphere* **2019**, *15*, 1066–1101. [[CrossRef](#)]
38. Ludwig, K.R. Isoplot v. 3.75—a geochronological toolkit for Microsoft Excel. In *Berkeley Geochronology Center Special Publication*; Berkeley Geochronology Center: Berkeley, CA, USA, 2012; Volume 5, pp. 1–75.
39. Smith, D.G. *Meandering River Point Bar Lithofacies Models: Modern and Ancient Examples Compared*; Ethridge, F.G., Flores, R.M., Harvey, M.D., Eds.; SEPM Special Publication: Tulsa, OK, USA, 1997; Volume 39, pp. 83–91.
40. McCarthy, P.J.; Martini, I.P.; Leckie, D.A. Anatomy and evolution of a Lower Cretaceous alluvial plain: Sedimentology and palaeosols in the upper Blairmore Group, south-western Alberta, Canada. *Sedimentology* **1997**, *44*, 197–220. [[CrossRef](#)]
41. Coleman, J.M. Ecological changes in a massive fresh-water clay sequence. *Trans. Gulf Coast Assoc. Geol. Soc.* **1966**, *16*, 159–174. [[CrossRef](#)]
42. Perez-Arlucea, M.; Smith, N.D. *Abstract: Proceedings of the 18th IAS Regional European Meeting of Sedimentology, Heidelberg, Germany, 2–4 September 1997*; IAS: Heidelberg, Germany, 1997; Volume 204, pp. 269–270.
43. Bridge, J.S. Large-scale facies sequences in alluvial overbank environments. *J. Sediment. Petrol.* **1984**, *54*, 583–588.
44. Ten Brinke, W.B.M.; Schoor, M.R.; Sorber, A.M.; Berendsen, H.J.A. Overbank sand deposition in relation to transport volumes during large-magnitude floods in the Dutch sand-bed Rhine river system. *Earth Surf. Process. Landf.* **1998**, *23*, 809–824. [[CrossRef](#)]
45. Smith, N.D.; Perez-Arlucea, M. Fine-grained splay deposition in the avulsion belt of the lower Saskatchewan River, Canada. *J. Sediment. Res.* **1994**, *B64*, 159–168.
46. Smith, D.G.; Smith, N.D. Sedimentation in anastomosed river systems; examples from alluvial valleys near Banff, Alberta. *J. Sediment. Petrol.* **1980**, *50*, 157–164. [[CrossRef](#)]
47. Retallack, G.J. *Soils of the Past: An Introduction to Paleopedology*, 2nd ed.; Blackwell Scientific Publishers: Oxford, UK, 2001.
48. McCarthy, P.J.; Martini, I.P.; Leckie, D.A. Use of micromorphology for palaeoenvironmental interpretation of complex alluvial palaeosols: An example from the Mill Creek Formation (Albian), southwestern Alberta, Canada. *Palaeogeogr. Palaeoclimatol. Palaeoecol.* **1998**, *143*, 87–110. [[CrossRef](#)]
49. Kraus, M.J. Paleosols in clastic sedimentary rocks: Their geologic applications. *Earth Sci. Rev.* **1999**, *47*, 41–70. [[CrossRef](#)]
50. McCarthy, P.J. Micromorphology and development of interfluvial paleosols: A case study from the Cenomanian Dunvegan Formation, NE British Columbia, Canada. *Bull. Can. Pet. Geol.* **2002**, *50*, 158–177. [[CrossRef](#)]
51. Spicer, R.A.; Parrish, J.T.; Grant, P.R. Controls on the Distribution and Quality of Cretaceous Coals. In *Geological Society of America Special Paper*; McCabe, P.J., Parrish, J.T., Eds.; Geological Society of America: Boulder, CO, USA, 1992; Volume 267, pp. 177–192.
52. Fiorillo, A.R. *Alaska Dinosaurs: An Ancient Arctic World*; CRC Press: Boca Raton, FL, USA, 2018.
53. Alexander, R. McN. Estimates of speeds of dinosaurs. *Nature* **1976**, *261*, 129–130. [[CrossRef](#)]
54. Henderson, D. Footprints, trackways, and hip heights of bipedal dinosaurs—testing hip height predictions with computer models. *Ichnos* **2003**, *10*, 99–114. [[CrossRef](#)]
55. Fiorillo, A.R.; Tykoski, R.S. Small hadrosaur manus and pes tracks from the Lower Cantwell Formation (Upper Cretaceous) Denali National Park, Alaska: Implications for locomotion in juvenile hadrosaurs. *Palaios* **2016**, *31*, 479–482. [[CrossRef](#)]

56. Seebacher, F. A new method to calculate allometric length-mass relationships of dinosaurs. *J. Vertebr. Paleontol.* **2001**, *21*, 51–60. [[CrossRef](#)]
57. Nesbitt, S.J.; Denton, R.K., Jr.; Loewen, M.A.; Brusatte, S.L.; Smith, N.D.; Turner, A.H.; Kirkland, J.L.; McDonald, A.T.; Wolfe, D.G. A mid-Cretaceous tyrannosauroid and the origin of North American end-Cretaceous dinosaur assemblages. *Nat. Ecol. Evol.* **2019**, *3*, 892–899. [[CrossRef](#)]
58. Brusatte, S.L.; Averianov, A.; Sues, H.D.; Muir, A.; Butler, I.B. New tyrannosaur from the mid-Cretaceous of Uzbekistan clarifies evolution of giant body sizes and advanced senses in tyrant dinosaurs. *Proc. Natl. Acad. Sci. USA* **2016**, *113*, 3447–3452. [[CrossRef](#)]
59. Rezendes, P. *Tracking and the Art of Seeing: How to Read Animal Tracks and Sign*, 2nd ed.; Harper Collins Publishers: New York, NY, USA, 1999.
60. Elbroch, M.; Marks, E. *Bird Tracks and Sign*; Stackpole Books: Mechanicsburg, PA, USA, 2001.
61. Currie, P.J. Bird footprints from the Gething Formation (Aptian, Lower Cretaceous) of northeastern British Columbia, Canada. *J. Vertebr. Paleontol.* **1981**, *1*, 257–264. [[CrossRef](#)]
62. Mehl, M.G. Additions to the vertebrate record of the Dakota Sandstone. *Am. J. Sci.* **1931**, *21*, 441–452. [[CrossRef](#)]
63. Lockley, M.; Chin, K.; Houck, K.; Matsukawa, M.; Kukihara, R. New interpretations of *Ignotornis*, the first-reported Mesozoic avian footprints: Implications for the paleoecology and behavior of an enigmatic Cretaceous bird. *Cretac. Res.* **2009**, *30*, 1041–1061. [[CrossRef](#)]
64. Fiorillo, A.R.; Hasiotis, S.T.; Kobayashi, Y.; Breithaupt, B.H.; McCarthy, P.J. Bird tracks from the Upper Cretaceous Cantwell Formation of Denali National Park, Alaska, USA: A new perspective on ancient northern polar vertebrate biodiversity. *J. Syst. Palaeontol.* **2011**, *9*, 33–49. [[CrossRef](#)]
65. Kang, S.H.; Buckley, L.G.; McCrea, R.T.; Kim, K.S.; Lockley, M.G.; Lim, J.D.; Lim, H.S.; Kim, C.B. First report of bird tracks (*Ignotornis seoungjoseoi* ichnosp. nov.) from the Jinju Formation (Lower Cretaceous), Sacheon City, Korea. *Cretac. Res.* **2021**, *127*, 104899. [[CrossRef](#)]
66. Currie, P.; Badamgarav, D.; Koppelhus, E. The first Late Cretaceous footprints from the Nemegt locality in the Gobi of Mongolia. *Ichnos* **2003**, *10*, 1–13. [[CrossRef](#)]
67. Lockley, M.G.; Nadon, G.; Currie, P.J. A diverse dinosaur-bird footprint assemblage from the Lance Formation, Upper Cretaceous, eastern Wyoming: Implications for ichnotaxonomy. *Ichnos* **2004**, *11*, 229–249. [[CrossRef](#)]
68. Fiorillo, A.R.; Hasiotis, S.T.; Kobayashi, Y. Herd structure in Late Cretaceous polar dinosaurs: A remarkable new dinosaur tracksite, Denali National Park, Alaska, USA. *Geology* **2014**, *42*, 719–722. [[CrossRef](#)]
69. Diaz-Martinez, I.; Pereda-Suberbiola, X.; Perez-Lorente, F.; Canudo, J.I. Ichnotaxonomic review of large ornithopod dinosaur tracks: Temporal and geographic implications. *PLoS ONE* **2015**, *10*, e0115477. [[CrossRef](#)] [[PubMed](#)]
70. Fiorillo, A.R.; Parrish, J.T. The first record of a Cretaceous dinosaur from southwestern Alaska. *Cretac. Res.* **2004**, *25*, 453–458. [[CrossRef](#)]
71. Fiorillo, A.R.; Adams, T.L.; Kobayashi, Y. New sedimentological, palaeobotanical, and dinosaur ichnological data on the palaeoecology of an unnamed Late Cretaceous rock unit in Wrangell-St. Elias National Park and Preserve, Alaska, USA. *Cretac. Res.* **2012**, *37*, 291–299. [[CrossRef](#)]
72. Fanti, F.; Bell, P.R.; Sissons, R.L. A diverse, high-latitude ichnofauna from the Late Cretaceous Wapiti Formation, Alberta, Canada. *Cretac. Res.* **2013**, *41*, 256–269. [[CrossRef](#)]
73. Lee, Y.N. Bird and dinosaur footprints in the Woodbine Formation (Cenomanian), Texas. *Cretac. Res.* **1997**, *18*, 849–864. [[CrossRef](#)]
74. Xing, L.; Lockley, M.G.; Kim, K.S.; Klein, H.; Matsukawa, M.; Lim, J.D.; Persons, W.S.; Xu, X. Mid-Cretaceous dinosaur track assemblage from the Tongfosi Formation of China: Comparison with the track assemblage of South Korea. *Cretac. Res.* **2017**, *74*, 155–164. [[CrossRef](#)]
75. McCrea, R.T.; Lockley, M.G.; Meyer, C.A. *The Armored Dinosaurs*; Carpenter, K., Ed.; Indiana University Press: Bloomington, IN, USA, 2001; pp. 413–454.
76. Riguetti, F.; Citton, P.; Apesteguía, S.; Zacarías, G.G.; Pereda-Suberbiola, X. New ankylosaurian trackways (cf. Tetrapodosaurus) from an uppermost Cretaceous level of the El Molino Formation of Bolivia. *Cretac. Res.* **2021**, *124*, 104810. [[CrossRef](#)]
77. Gangloff, R.A. *Edmontonia* sp., the first record of an ankylosaur from Alaska. *J. Vertebr. Paleontol.* **1995**, *15*, 195–200. [[CrossRef](#)]
78. Godefroit, P.; Golovneva, L.; Shchepetov, S.; Garcia, G.; Alekseev, P. The last polar dinosaurs: High diversity of latest Cretaceous arctic dinosaurs in Russia. *Naturwissenschaften* **2009**, *96*, 495–501. [[CrossRef](#)] [[PubMed](#)]
79. Kohn, M.J. Carbon isotope compositions of terrestrial C3 plants as indicators of (paleo) ecology and (paleo) climate. *Proc. Natl. Acad. Sci. USA* **2010**, *107*, 19691–19695. [[CrossRef](#)] [[PubMed](#)]
80. Diefendorf, A.F.; Mueller, K.E.; Wing, S.L.; Koch, P.L.; Freeman, K.H. Global patterns in leaf ^{13}C discrimination and implications for studies of past and future climate. *Proc. Natl. Acad. Sci. USA* **2010**, *107*, 5738–5743. [[CrossRef](#)]
81. Leavitt, S.W.; Long, A. Stable-carbon isotope variability in tree foliage and wood. *Ecology* **1986**, *67*, 1002–1010. [[CrossRef](#)]
82. Ciesielczuk, J.; Górká, M.; Fabiańska, M.J.; Misz-Kennan, M.; Jura, D. The influence of heating on the carbon isotope composition, organic geochemistry and petrology of coal from the Upper Silesian Coal Basin (Poland): An experimental and field study. *Int. J. Coal Geol.* **2021**, *241*, 103749. [[CrossRef](#)]
83. Barral, A.; Gomez, B.; Legendre, S.; Lécuyer, C. Evolution of the carbon isotope composition of atmospheric CO_2 throughout the Cretaceous. *Palaeogeogr. Palaeoclimatol. Palaeoecol.* **2017**, *471*, 40–47. [[CrossRef](#)]

84. Poulsen, C.J.; Pollard, D.; White, T.S. General circulation model simulation of the $\delta^{18}\text{O}$ content of continental precipitation in the middle Cretaceous: A model-proxy comparison. *Geology* **2007**, *35*, 199–202. [[CrossRef](#)]
85. Suarez, M.B.; González, L.A.; Ludvigson, G.A. Quantification of a greenhouse hydrologic cycle from equatorial to polar latitudes: The mid-Cretaceous water bearer revisited. *Palaeogeogr. Palaeoclimatol. Palaeoecol.* **2011**, *307*, 301–312. [[CrossRef](#)]
86. Gangloff, R.A. Arctic dinosaurs with emphasis on the Cretaceous record of Alaska and the Eurasian-North American connection. *New Mex. Mus. Nat. Hist. Sci. Bull.* **1998**, *14*, 211–220.
87. Roehler, H.W.; Stricker, G.D. Dinosaur and wood fossils from the Cretaceous Corwin Formation in the National Petroleum Reserve, north slope of Alaska. *J. Alsk. Geol. Soc.* **1984**, *4*, 35–41.
88. Parrish, J.M.; Parrish, J.T.; Hutchison, J.H.; Spicer, R.A. Late Cretaceous vertebrate fossils from the North Slope of Alaska and implications for dinosaur ecology. *Palaios* **1987**, *2*, 377–389. [[CrossRef](#)]
89. Lease, R.O.; Houseknecht, D.W.; Kylander-Clark, A.R. Quantifying large-scale continental shelf margin growth and dynamics across middle-Cretaceous Arctic Alaska with detrital zircon U-Pb dating. *Geology* **2022**, *50*, 620–625. [[CrossRef](#)]
90. Fiorillo, A.R.; Kobayashi, Y.; McCarthy, P.J.; Tanaka, T.; Tykoski, R.S.; Lee, Y.N.; Takasaki, R.; Yoshida, J. Dinosaur ichnology and sedimentology of the Chignik Formation (Upper Cretaceous), Aniakchak National Monument, southwestern Alaska; Further insights on habitat preferences of high-latitude hadrosaurs. *PLoS ONE* **2019**, *14*, e0223471. [[CrossRef](#)] [[PubMed](#)]
91. McCrea, R.T.; Buckley, L.G.; Currie, P.J.; Plint, A.G.; Helm, C.W.; Haggart, J.W. A review of vertebrate track-bearing formations from the Mesozoic and earliest Cenozoic of western Canada with a description of a new theropod ichnospecies and reassignment of an avian ichnogenus. *New Mex. Mus. Nat. Hist. Sci. Bull.* **2014**, *62*, 5–94.
92. Bamforth, E. Exploring the Role of Evolving Forest Composition in Shaping Dinosaur Diversity Patterns in the Cretaceous of Northern Alberta, Canada. In Proceedings of the Society of Vertebrate Paleontology Annual Meeting, Cincinnati, OH, USA, 18–21 October 2023; pp. 81–82.
93. Bart, J.R.; Johnston, V.H. *Arctic shorebirds in North America: A Decade of Monitoring*; University of California Press: Berkeley, CA, USA, 2012.
94. Lawver, L.A.; Grantz, A.; Gahagan, L.M. Tectonic Evolution of the Bering Shelf–Chukchi Sea–Arctic Margin and Adjacent Landmasses. In *Geological Society of America Special Paper*; Miller, E.L., Grantz, A., Klemperer, S.L., Eds.; Geological Society of America: Boulder, CO, USA, 2002; Volume 360, pp. 333–358.

Disclaimer/Publisher’s Note: The statements, opinions and data contained in all publications are solely those of the individual author(s) and contributor(s) and not of MDPI and/or the editor(s). MDPI and/or the editor(s) disclaim responsibility for any injury to people or property resulting from any ideas, methods, instructions or products referred to in the content.